Air-Induced PIM Cancellation in FDD MIMO Transceivers

Vesa Lampu, *Graduate Student Member, IEEE*, Lauri Anttila, *Member, IEEE*, Matias Turunen, Marko Fleischer, Jan Hellmann, and Mikko Valkama, *Fellow, IEEE*

***Abstract*— In this letter, air-induced passive intermodulation (PIM) modeling and cancellation schemes are presented in a multiple-input multiple-output (MIMO) frequency-division duplexing (FDD) transceiver context. PIM is distortion generated by nonlinear passive devices either within the transmitter chain or outside the transceiver system, as is the case in air-induced PIM. In FDD systems, the PIM products may lie on the receiver band, thus possibly desensitizing the receiver chain. Unlike previous PIM cancellation works, we consider a challenging rank-2 dual-carrier MIMO transceiver scenario, with two spatially multiplexed signals per component carrier (CC). Stemming from the PIM modeling, we first present a cancellation method based on a complete set of identified basis functions (BFs). Additionally, to relax the processing complexity, we propose an alternative canceller solution with a reduced number of BFs, inspired by the problem modeling. RF measurements conducted with real-life equipment indicate favorable PIM suppression levels of up to 20 dB using both introduced techniques.**

***Index Terms*— 5G, carrier aggregation (CA), duplexing, interference cancellation, nonlinear systems, passive intermodulation (PIM).**

I. Introduction

CARRIER aggregation (CA) technology was introduced in long-term evolution (LTE)-advanced and is also being included in the current 5G New Radio (NR) specifications [1]. In CA, multiple component carriers (CCs) are adopted to increase throughput and capacity, while, in general, the CC allocation can be contiguous or noncontiguous in frequency. When such CA signals experience nonlinearity—especially in the case of noncontiguous allocation—severe intermodulation distortion can be generated, and if the source of the nonlinearity is a passive device, the distortion is called passive intermodulation (PIM) [2]–[8]. PIM can, in general, be generated by loose connection of cables, filters, switches, or even external metallic objects in the radiation field of the antennas, which we call air-induced PIM in this work.

For certain frequency range (FR)-1 bands, such as band n3, the 5G NR specifications determine the use of frequency-division duplexing (FDD). In such FDD networks, the transmission and reception are simultaneous, but occur on different frequencies. Thus, as illustrated in Fig. 1, PIM may easily present an issue since the PIM products can fall on the receiver (RX) operating frequency possibly desensitizing the RX path. This is particularly so when the duplexing distance is small, as is the case, for example, with NR band n3. An obvious solution to the problem is to use components that do not produce PIM, but these increase the manufacturing costs of the devices [2]. Additionally, in certain air-induced PIM scenarios, the source can be part of the built environment around the transceiver antenna system and thus might be impossible to remove from the radiation field. Therefore, the development of efficient PIM suppression techniques is an important topic of both scientific and practical relevance.

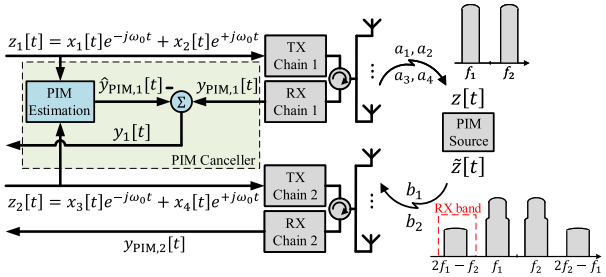

Fig. 1. Simplified block diagram of the considered system, with two TX/RX chains and a PIM source located in the base-station radiation field. Also, some basic modeling-related notations are shown.

To this end, the early work in [2] introduced a nonlinear imposer network, showing up to 40 dB of PIM suppression. Also in the analog domain, the work in [3] demonstrated PIM mitigation methods by introducing a compensation signal or an additional passive PIM source accompanied by a phase shifter in simulations. In [4], a tunable nonlinear transmission line strip to cancel PIM was introduced. The work in [5] considered a completely digital solution for conducted PIM building upon the third-order basis functions (BFs) of a two CC system. In [6], the second-order PIM products of a diplexer were modeled by BFs and suppressed. More recently, in [7], conducted PIM cancellers taking into account also the potentially co-existing PA nonlinearity with reduced complexity through decoupling the memory were introduced, focusing also on a two CC case. Our previous work [8] considered the modeling and digital cancellation of air-induced PIM in a simple two CC scenario.

In this letter, we extend our previous work [8] focusing on air-induced PIM. Unlike prior art, we consider a challenging rank-2 dual-carrier multiple-input multiple-output (MIMO) FDD system where four CCs are transmitted simultaneously, illustrated in Fig. 1. Although the PIM issue in MIMO has been mentioned in the literature, for example, in [9]–[11],

Manuscript received February 25, 2022; revised March 29, 2022; accepted March 30, 2022. Date of publication April 15, 2022; date of current version June 7, 2022. This work was supported in part by Nokia Mobile Networks and in part by the Academy of Finland under Grant 319994, Grant 323461, and Grant 338224. *(Corresponding author: Vesa Lampu.)*

Vesa Lampu, Lauri Anttila, Matias Turunen, and Mikko Valkama are with the Department of Electrical Engineering, Tampere University, FI-33720 Tampere, Finland (e-mail: vesa.lampu@tuni.fi).

Marko Fleischer and Jan Hellmann are with Nokia Mobile Networks, 89081 Ulm, Germany.

This article was presented at the IEEE MTT-S International Microwave Symposium (IMS 2022), Denver, CO, USA, June 19–24, 2022.

Color versions of one or more figures in this letter are available at https://doi.org/10.1109/LMWC.2022.3164718.

Digital Object Identifier 10.1109/LMWC.2022.3164718

to the best of the authors' knowledge, this is the first work to model and cancel PIM in the MIMO context where more than two CCs are employed, which clearly complicates the modeling and the corresponding digital cancellation as shown in the letter. To alleviate the increased complexity, we propose a novel, yet simple method to limit the computational complexity, based on the physical modeling of the system. The models are then validated through RF measurements at 5G NR band n3 with true base-station hardware, evidencing excellent PIM suppression capabilities.

II. Proposed Methods

Here, we introduce the air-induced PIM modeling as well as two new PIM suppression methods in a dual-carrier rank-2 MIMO FDD context, where four physical CCs are transmitted. The considered system is illustrated in Fig. 1.

A. Complete BF Method

We model the physical RF system through baseband (BB) equivalent approach such that the CCs $x_1[t]$ and $x_3[t]$ appear at $-\omega_0$ and CCs $x_2[t]$ and $x_4[t]$ at $+\omega_0$, while the corresponding true RF frequencies are f_1 and f_2, respectively, as depicted in Fig. 1. Furthermore, two physical TX chains are considered, for rank-2 transmission per frequency resource, as also shown in Fig. 1. As the air-PIM source is anyway in close vicinity of the radiating antenna system, we assume slow-varying line-of-sight (LOS)-type channels with frequency flat responses between the air-PIM source and the TX and RX antenna system(s). Therefore, the total air-combined signal $z[t]$ at the PIM source input can be written as

$$z[t] = (a_1x_1[t] + a_3x_3[t])e^{-j\omega_0 t} + (a_2x_2[t] + a_4x_4[t])e^{+j\omega_0 t} \tag{1}$$

where the coefficient a denotes the beamformed channel response from TX antennas to the PIM source for each CC. This signal then undergoes a nonlinear transformation in the PIM source, modeled here by a memory polynomial (MP) model [12], producing

$$\tilde{z}[t] = \sum_{m=-M_1}^{M_2} \sum_{\substack{p=1 \\ p \text{ odd}}}^{P} g_{p,m} z[t-m]|z[t-m]|^{p-1} \tag{2}$$

where M_1 and M_2 denote the number of precursor and postcursor taps, respectively, P is the polynomial order, and g denotes the MP model coefficients. Assuming then that the RX band appears at the intermodulation frequency $2f_1 - f_2$ and denoting the corresponding channel response from the PIM source to the considered RX by b, the received PIM signal can be expressed as in (3), as shown at the bottom of this page, where only the third polynomial order ($p = 3$) BFs are shown for illustration simplicity. By lumping the total coefficients of each BF to c, the received PIM signal can be written as in (4), as shown at the bottom of this page.

Since the samples of the signals $x_i[t]$ are known, the model in (4) allows for air-induced PIM cancellation, assuming that the involved unknown c coefficients are first estimated. Due to the linear-in-parameters nature of the model in (4), least-squares (LS) estimation is a straightforward approach. The estimated coefficients and the known CC samples are then used to construct a PIM cancellation signal, $\hat{y}_{\text{PIM}}[t]$, which as highlighted in Fig. 1 is subtracted from the actual received signal to suppress PIM. This is done in parallel in both RXs with separate parameter estimators and cancellation signals.

However, the computational complexity of this approach rises very rapidly with increasing polynomial orders, as there are 6 instantaneous BFs for polynomial order 3, and already 34 for order 5. Complexity is further increased when memory is considered in the model. To address such a challenge, we next propose an alternative method to decrease the complexity while maintaining excellent modeling accuracy.

B. Channel Coefficient Method

The number of BFs required to calculate real-time PIM samples can be reduced by generating the BFs from two aggregated signals, $v_1[t]$ and $v_2[t]$, instead of the four individual CC signals considered before. This is stemming from (1), and we specifically define $v_1[t] = d_1x_1[t] + x_3[t]$ and $v_2[t] = d_2x_2[t] + x_4[t]$ such that the signals v consider the relative amplitudes and phases of the CCs at the nonlinearity input, denoted by complex values $d_1 = a_1/a_3$ and $d_2 = a_2/a_4$. To this end, it can be deduced from (3) and (4) that these complex numbers can be written by utilizing the coefficients of the instantaneous ($m = 0$) third-order BFs as

$$d_1 = \frac{2c_1}{c_2} = \frac{c_2}{2c_3} = \pm\sqrt{\frac{c_1}{c_3}} = \frac{2c_4}{c_5} = \frac{c_5}{2c_6} = \pm\sqrt{\frac{c_4}{c_6}} \tag{5}$$

$$d_2 = \frac{c_1^*}{c_4^*} = \frac{c_2^*}{c_5^*} = \frac{c_3^*}{c_6^*}. \tag{6}$$

After the coefficients d are estimated using the instantaneous third-order BFs of (4), a more complete received PIM model can then be constructed, following the MP approach, as

$$\begin{aligned} y_{\text{PIM}}[t] = \sum_{m=-M_1}^{M_2} & h_{1,m} v_1[t-m]^2 v_2[t-m]^* \\ & + h_{2,m} v_1[t-m]^2 v_2[t-m]^* |v_1[t-m]|^2 \\ & + h_{3,m} v_1[t-m]^2 v_2[t-m]^* |v_2[t-m]|^2 + \cdots \end{aligned} \tag{7}$$

where h is the total lumped coefficient of each BF. Utilizing this model, there is only 1 instantaneous BF for polynomial order 3, and 2 for order 5, promising a great reduction

$$\begin{aligned} y_{\text{PIM}}[t] = b \sum_{m=-M_1}^{M_2} & a_1^2 a_2^* g_{3,m} x_1[t-m]^2 x_2[t-m]^* + 2a_1 a_3 a_2^* g_{3,m} x_1[t-m] x_3[t-m] x_2[t-m]^* + a_3^2 a_2^* g_{3,m} x_3[t-m]^2 x_2[t-m]^* \\ & + a_1^2 a_4^* g_{3,m} x_1[t-m]^2 x_4[t-m]^* + 2a_1 a_3 a_4^* g_{3,m} x_1[t-m] x_3[t-m] x_4[t-m]^* + a_3^2 a_4^* g_{3,m} x_3[t-m]^2 x_4[t-m]^* + \cdots \end{aligned} \tag{3}$$

$$\begin{aligned} y_{\text{PIM}}[t] = \sum_{m=-M_1}^{M_2} & c_{1,m} x_1[t-m]^2 x_2[t-m]^* + c_{2,m} x_1[t-m] x_3[t-m] x_2[t-m]^* + c_{3,m} x_3[t-m]^2 x_2[t-m]^* \\ & + c_{4,m} x_1[t-m]^2 x_4[t-m]^* + c_{5,m} x_1[t-m] x_3[t-m] x_4[t-m]^* + c_{6,m} x_3[t-m]^2 x_4[t-m]^* + \cdots \end{aligned} \tag{4}$$

Fig. 2. Measurement setup with the relevant parts of the system highlighted.

in computational complexity compared to the complete BF approach described in the previous section.

It is noted that this simplified method requires the application of LS-type parameter estimation twice—rather than once as in the complete BF case—since the coefficients d need to be determined first. However, the estimation of the d coefficients can be offloaded to another part of the system running in parallel to the actual estimation and cancellation engine that builds on (7). Assuming slow-varying air-PIM channels, the required update interval for the coefficient d is also likely to be relatively long, while the actual real-time cancellation engine benefits from the largely reduced complexity of the expression in (7) compared to (4).

III. RF Measurements and Results

The measurement setup is depicted in Fig. 2. A dual-TX/RX base-station entity with directive antenna systems, similar to the one shown in Fig. 1, is placed in an anechoic chamber along with a test PIM source. In the measurements, standard off-the-shelf steel wool is used as a PIM source, which lies a meter away from the antennas. The radio device is controlled by a PC located outside the chamber. The PC also collects data from the radio for post-processing.

The proposed methods are tested with two TX signal bandwidths (BWs), 5 and 20 MHz. Both TX chains transmit two 5G NR standard-compliant CP-OFDM signals as the CCs, with the chosen BW. The individual carriers lie at 5G NR band n3, at TX frequencies of 1819.0 and 1866.5 MHz in both the TX chains, while the RX frequency in both RX chains is set to 1771.5 MHz, which corresponds to the lower third-order intermodulation frequency of the chosen TX frequencies. All the carriers were transmitted with +31 dBm output power plus the antenna gain.

The original BB sampling rate of the transmitted CCs is 7.68 MHz for the 5 MHz BW and 30.72 MHz for the 20 MHz BW. For the BF generation, the signals are upsampled by a factor of 16. The canceller solutions consider polynomial orders up to five ($P = 5$), and five taps of memory such that $M_1 = M_2 = 2$. Therefore, the complete BF model incorporates 200 BFs, while the channel coefficient method includes only 15 BFs, plus the six additional BFs to estimate the coefficient d. Thus, the total number of parameters with the channel coefficient method is 21.

Fig. 3 shows the measured cancellation results, using data measured from RX chain 1. Results from RX chain 2 are very similar. A channel selection filter at the RX side limits the BW of the measured signals to the chosen signal BW. In the 5 MHz case, the received PIM signal is approximately 22 dB above the noise floor, and both of the canceled signals are only

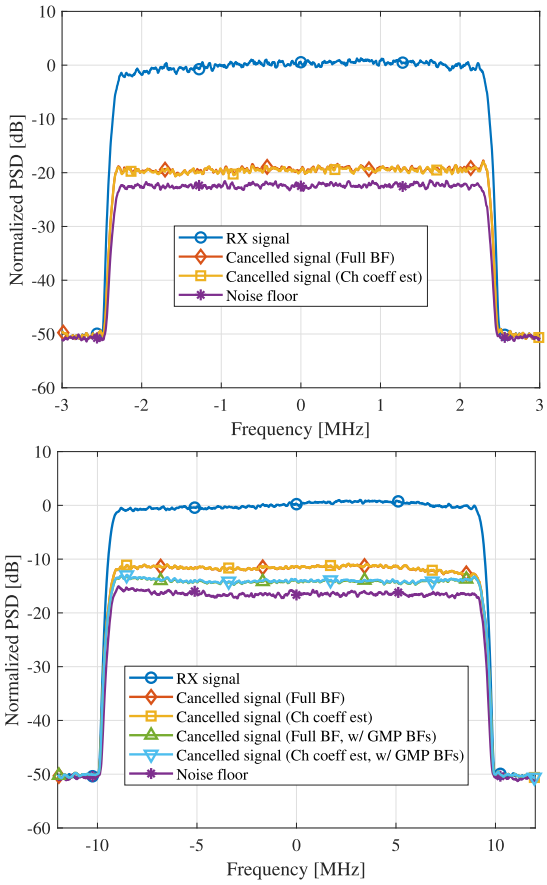

Fig. 3. Measured cancellation results for the two considered models, utilizing 5G NR compliant 5 MHz (upper) and 20 MHz (lower) BW CP-OFDM signals at NR band n3.

some 2 dB from the noise floor. Therefore, both the complete BF and the channel coefficient methods are able to cancel around 20 dB of the air-induced PIM. In the 20 MHz case, the PIM level is around 16.5 dB above the noise floor, and both cancellers suppress the PIM by some 11.5 dB, leaving a residual of 5 dB. For higher modeling fidelity, additional BFs can be utilized in the cancellation stage. As an example, adding two leading and two lagging envelope BFs of the third-order generalized MP (GMP) model [13], both cancellers suppress the PIM levels by 14 dB, leaving a residual of 2.5 dB. With these added BFs, the complete model employs 232 BFs, while the channel coefficient model merely 25, counting the six required by d parameters. These results highlight the accuracy of the introduced complete model, which can also be maintained with much reduced complexity with the channel coefficient estimation method. The existing methods from [5]–[8] are not shown as they cannot handle the coexistence of four simultaneous signals.

IV. Conclusion

A model for air-induced PIM in a dual-carrier rank-2 MIMO FDD transceiver with four CCs was introduced in this letter. Based on the model, prediction and cancellation of the received PIM samples can be achieved. Due to the high number of involved BFs, a reduced complexity method utilizing the air-PIM-related channel coefficients was also proposed. Measurements made with real-life instruments indicate that both the complete BF and the channel coefficient methods achieve similar PIM suppression levels, capable of canceling the measured PIM by up to 20 dB.

REFERENCES

[1] *NR; Base Station (BS) Radio Transmission and Reception*, document 38.104 v15.9.0, 3GPP, Apr. 2020.

[2] J. Henrie, A. Christianson, and W. J. Chappell, "Cancellation of passive intermodulation distortion in microwave networks," in *Proc. 38th Eur. Microw. Conf.*, 2008, pp. 1153–1156.

[3] Q. Jin, J. Gao, H. Huang, and L. Bi, "Mitigation methods for passive intermodulation distortion in circuit systems using signal compensation," *IEEE Microw. Wireless Compon. Lett.*, vol. 30, no. 2, pp. 205–208, Feb. 2020.

[4] X. Chen, T. Ren, D. J. Pommerenke, and M. Yu, "Broadband mechanical intermodulation tuner using reconfigurable distributed nonlinearity," *IEEE Trans. Microw. Theory Techn.*, vol. 70, no. 1, pp. 5–13, Jan. 2022.

[5] H.-T. Dabag, H. Gheidi, S. Farsi, P. Gudem, and P. M. Asbeck, "All-digital cancellation technique to mitigate receiver desensitization in uplink carrier aggregation in cellular handsets," *IEEE Trans. Microw. Theory Techn.*, vol. 61, no. 12, pp. 4754–4765, Dec. 2013.

[6] H. Gheidi, H.-T. Dabag, Y. Liu, P. M. Asbeck, and P. Gudem, "Digital cancellation technique to mitigate receiver desensitization in cellular handsets operating in carrier aggregation mode with multiple uplinks and multiple downlinks," in *Proc. IEEE Radio Wireless Symp. (RWS)*, Jan. 2015, pp. 221–224.

[7] M. Z. Waheed *et al.*, "Passive intermodulation in simultaneous transmit–receive systems: Modeling and digital cancellation methods," *IEEE Trans. Microw. Theory Techn.*, vol. 68, no. 9, pp. 3633–3652, Sep. 2020.

[8] V. Lampu, L. Anttila, M. Turunen, M. Fleischer, J. Hellmann, and M. Valkama, "Air-induced passive intermodulation in FDD networks: Modeling, cancellation and measurements," in *Proc. 55th Asilomar Conf. Signals, Syst., Comput.*, 2021, pp. 983–988.

[9] J.-B. Yan, S. Yong, and J. T. Bernhard, "Intermodulation and harmonic distortion in frequency reconfigurable slot antenna pairs," *IEEE Trans. Antennas Propag.*, vol. 62, no. 3, pp. 1138–1146, Mar. 2014.

[10] S. Akoum and J. Acharya, "Full-dimensional MIMO for future cellular networks," in *Proc. IEEE Radio Wireless Symp. (RWS)*, Dec. 2014, pp. 1–3.

[11] E. Björnson, M. Matthaiou, and M. Debbah, "Massive MIMO with non-ideal arbitrary arrays: Hardware scaling laws and circuit-aware design," *IEEE Trans. Wireless Commun.*, vol. 14, no. 8, pp. 4353–4368, Aug. 2015.

[12] L. Ding *et al.*, "A robust digital baseband predistorter constructed using memory polynomials," *IEEE Trans. Commun.*, vol. 52, no. 1, pp. 159–165, Jan. 2004.

[13] D. R. Morgan, Z. Ma, J. Kim, M. G. Zierdt, and J. Pastalan, "A generalized memory polynomial model for digital predistortion of RF power amplifiers," *IEEE Trans. Signal Process.*, vol. 54, no. 10, pp. 3852–3860, Oct. 2006.